

Auto-Control Technique Using Gradient Method Based on Radial Basis Function Neural Networks to Control of an Activated Sludge Process of Wastewater Treatment



Abdallah Lemita¹, Sebti Boulahbel¹, Sami Kahla^{2*}, Moussa Sedraoui³

¹ Department of Electronics, Faculty of Engineering, University Ferhat Abbas Setif 1, Setif 19000, Algeria

² Research Center in Industrial Technologies, CRTI, P.O. Box 64, Cheraga, Algiers 16014, Algeria

³ Telecommunication Laboratory, University 8 Mai 1945, Guelma 24000, Algeria

Corresponding Author Email: samikahla40@yahoo.com

<https://doi.org/10.18280/jesa.530510>

ABSTRACT

Received: 20 December 2019

Accepted: 13 September 2020

Keywords:

activated sludge process, wastewater treatment, gradient descent algorithm, RBF neural network, PI control

Dissolved oxygen (DO) concentration is a key variable in the activated sludge wastewater treatment processes. In this paper, an auto control strategy based on Euler method and gradient method with radial basis function (RBF) neural networks (NNs) is proposed to solve the DO concentration control problem in an activated sludge process of wastewater treatment. The control purpose is to maintain the dissolved oxygen concentration in the aerated tank for having the substrate concentration within the standard limits established by legislation of wastewater treatment. For that reason, a new proposed control strategy based on gradient descent method and RBF neural network has been used. Compared with RBF neural network PI control, the obtained results show the effectiveness in terms of both transient and steady performances of proposed control method for dissolved oxygen control in the activated sludge wastewater treatment processes.

1. INTRODUCTION

The wastewater treatment process is a very complex process; it presents strong nonlinearity and uncertainties regarding to its parameters. The wastewater treatment comprises various steps used for reducing the contaminants in the wastewater which are: pretreatment, primary treatment, secondary treatment [1, 2]. The pretreatment has the objective of removing solid objects, and to skimming off floating greases and oils. Without passing the wastewater through the pretreatment, these objects may cause block and damage the equipment and the other steps of treatments. The primary treatment removes the remaining suspended and dissolved solids.

The secondary or biological treatment is the most important step of wastewater treatment. It aims to add microorganisms to reduce the organic matter, nitrogen and phosphorus from the wastewater. There are different methods used in the wastewater treatment process, but the most used and popular one is the activated sludge process (ASP) [3, 4].

In the last years, varieties of researches have been conducted about the control of the level of dissolved oxygen to enhance the process. In general, improvements are related to the controlling techniques. A linear proportional integral (PI) controller with feedforward from the flow rate and the respiration rate has been shown as a basic strategy [4]. Because of the PID controller limitation, the classical method of proportional integral derivative (PID) has been attempted, and the controlling effect of the dissolved oxygen is not satisfactory enough. However, the controllers are normally designed for the particular operational conditions because of the scarcity of sufficient hard or soft sensors and the nonlinear features of the bioprocesses [5]. In recent times, scholars have begun to study the artificial intelligence (AI) technologies

which can be widely implemented in numerous areas, including chemical and biochemical processes and. Due to its great capabilities and adaptabilities of nonlinear modelling, the most prevalent AI controlling strategies are neural network and fuzzy network, which are usually integrated with the PID control. A fuzzy method to the control of dissolved oxygen in the process of aeration was studied by Man et al. [6]. An adaptive fuzzy control strategy for dissolved oxygen concentration was used to control of an activated sludge process Liu et al. [7]. In the paper [8] an adaptive fuzzy neural network-based model predictive control (AFNN-MPC) is proposed for the control problem of DO concentration. Piotrowski proposed a supervisory heuristic fuzzy control system applied to a Sequencing Batch Reactor (SBR) in the Wastewater Treatment Plant (WWTP) [9]. Lin and Luo [10] developed an adaptive neural technique using a disturbance observer to solve the dissolved oxygen concentration control problem. An improved multi objective optimal control (MOOC) strategy is developed to improve the operational efficiency, satisfy the effluent quality (EQ) and reduce the energy consumption (EC) in wastewater treatment process [11]. Mirghasemi proposed a robust adaptive neural network control strategy and used it to control the dissolved oxygen in activated sludge process application [12].

In this paper, a control strategy based on Euler method and gradient method with RBF neural network is proposed to control the dissolved oxygen concentration in an activated sludge process of wastewater treatment. The Euler is a numerical method that is used to approximate the solution of a nonlinear differential equation (nonlinear system), and the gradient descent algorithm and the RBF neural network are used to find the values of a function's parameters (coefficients) that minimize a performance function as possible. The performance of the proposed control strategies laws is

illustrated with numerical simulations comparing their results with RBFNN-PI controller.

The remainder of this paper is organized as follows: in Section 2, Euler method is clearly discussed, in Section 3, presents a nonlinear control strategy based on gradient method accompanied with neural network method. In Section 4, RBF neural network PI control is discussed. The Section 5, a mathematical model of wastewater treatment process is given. In Section 6, the simulation results are presented. Finally, it is ended by a conclusion.

2. EULER METHOD

The Euler's method is numerical method that is used to approximate the solutions of a differential equation (Figure 1). Let consider the following differential equation:

$$\frac{\partial y(t)}{\partial t} = f(t, y(t)) \quad (1)$$

$\forall t \in \mathfrak{R}, y(0) = y_0$ is the initial condition.

t: time variable, y: output system.

The principal of Euler's method is to integrate the two parts of Eq. (1) between t_0 and t_1 .

$$\int_{t_0}^{t_1} \frac{\partial y(t)}{\partial t} dt = \int_{t_0}^{t_1} f(t, y(t)) dt \quad (2)$$

$$y(t_1) = y(t_0) + \int_{t_0}^{t_1} f(t, y(t)) dt \quad (3)$$

The integral $\int_{t_0}^{t_1} f(t, y(t)) dt$ can be approximated by:

* The area of upper rectangle of $f(t_0, y(t_0))$ and length $t_1 - t_0 = h$. Then:

$$\int_{t_0}^{t_1} f(t, y(t)) dt \approx h \cdot f(t_0, y(t_0)) \quad (4)$$

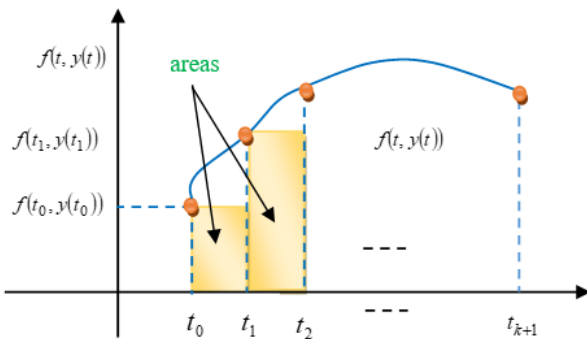


Figure 1. Euler method

* The area of upper rectangle of $f(t_1, y(t_1))$ and length $t_1 - t_0 = h$. Then:

$$\int_{t_0}^{t_1} f(t, y(t)) dt \approx h \cdot f(t_1, y(t_1)) \quad (5)$$

* The following statement results from the application of the trapezoidal rule in the approximation integration of the integral in Eq. (2).

$$\int_{t_0}^{t_1} f(t, y(t)) dt \approx \frac{h}{2} \cdot (f(t_0, y(t_0)) + f(t_1, y(t_1))) \quad (6)$$

By using Eq. (4), The numerical solution of Eq. (1) can be given by the following equation:

$$y(t_1) = y(t_0) + h \cdot f(t_0, y(t_0)) \quad (7)$$

For $k \geq 0$:

$$y(t_{k+1}) = y(t_k) + h \cdot f(t_k, y(t_k)) \quad (8)$$

Now, consider a nonlinear system that can be written as the following differential equation:

$$\frac{\partial y_u(t)}{\partial t} = f(t, y_u(t), u(t)) \quad (9)$$

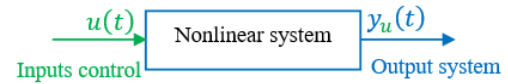


Figure 2. Nonlinear system with single input-single output

The curve of the output system $y_u(t_k)$ depends on the input control $u(t)$. If we consider two different inputs control $u(t)=u_0$, and $u(t)=u_1$, then Eq. (9) yields:

$$\frac{\partial y_{u_0}(t)}{\partial t} = f(t, y_{u_0}(t), u_0) \quad (10)$$

$$\frac{\partial y_{u_1}(t)}{\partial t} = f(t, y_{u_1}(t), u_1) \quad (11)$$

The numerical solutions of these equations (Eq. (10) and Eq. (11)) by using Euler's method are:

$$y_{u_0}(t_{k+1}) = y_{u_0}(t_k) + h \cdot f(t_k, y_{u_0}(t_k), u_0) \quad (12)$$

$$y_{u_1}(t_{k+1}) = y_{u_1}(t_k) + h \cdot f(t_k, y_{u_1}(t_k), u_1) \quad (13)$$

Figure 3 shows the curves of Eq. (12) and Eq. (13).

Figure 3 shows that if we apply two different inputs $u(t)=u_0$ and $u(t)=u_1$ on system in Figure 2, we will have two different trajectories in the output system. Suppose that we know the input $u(t)=u_0$, if we want that the trajectory $y_{u_0}(t_{k+1})$ (blue curve) tracks the trajectory $y_{u_1}(t_{k+1})$ (red curve), we have to find the value of input control u_1 that makes the trajectory y_{u_0} tracks the trajectory y_{u_1} .

The aim of the proposed control strategy is to control the system output $y_{u_0}(t_{k+1})$ to track a desired reference $r(t_{k+1})$ by changing at every instant t_k the value of input control u_k .

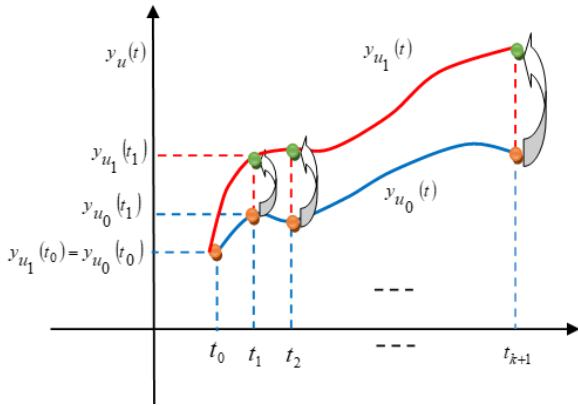


Figure 3. Curve of Eq. (9) with two different inputs control $u(t) = u_0$ and $u(t) = u_1$

3. GRADIENT DESCENT ALGORITHM BASED ON RBF NEURAL NETWORK

The proposed control strategy is depicted in Figure 4.

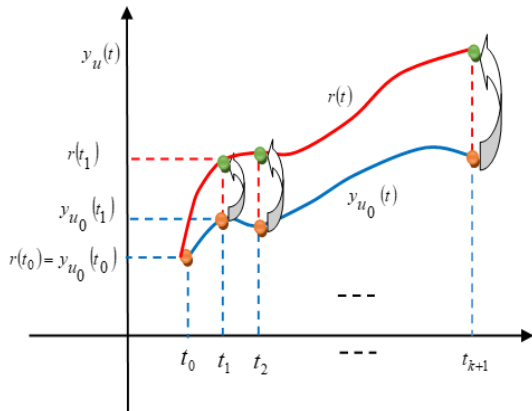


Figure 4. Curve of Principal of the proposed control strategy

Consider the following nonlinear system:

$$\frac{\partial y_{u_0}(t)}{\partial t} = f(t, y_{u_0}(t), u_0) \quad (14)$$

The numerical solution of Eq. (14) by using Euler's method is:

$$y_{u_0}(t_1) = y_{u_0}(t_0) + h \cdot f(t_0, y_{u_0}(t_0), u_0) \quad (15)$$

At time t_1 , we have to find the value of the input control u_1 to get: $y_{u_0}(t_1) = r(t_1)$.

$$y_{u_1}(t_1) = y_{u_0}(t_0) + h \cdot f(t_0, y_{u_0}(t_0), u_1) \quad (16)$$

The input control u_1 is adjusted by using the gradient descent algorithm by minimizing the performance function

with respect to u_0 . The performance function is the squared error $E(t_1)$ between $y_{u_1}(t_1)$ and $y_{u_0}(t_1)$.

$$E(t_1) = \frac{1}{2} (e(t_1))^2 = \frac{1}{2} (y_{u_1}(t_1) - y_{u_0}(t_1))^2 \quad (17)$$

$$E(t_1) = \frac{1}{2} (r(t_1) - y_{u_0}(t_1))^2 \quad (18)$$

Input control u_1 updating by using the gradient descent algorithm:

$$u_1 = u_0 + \Delta u_0 \quad (19)$$

$$\Delta u_0 = -\lambda \cdot \frac{\partial E(t_1)}{\partial u_0} \quad (20)$$

Then:

$$u_1 = u_0 - \lambda \cdot \frac{\partial E(t_1)}{\partial u_0} \quad (21)$$

where, λ : learning rate.

$$u_1 = u_0 - \lambda \cdot \frac{\partial E(t_1)}{\partial y_{u_0}(t_1)} \cdot \frac{\partial y_{u_0}(t_1)}{\partial f(t_0, y_{u_0}(t_0), u_0)} \cdot \frac{\partial f(t_0, y_{u_0}(t_0), u_0)}{\partial u_0} \quad (22)$$

$$u_1 = u_0 + \lambda \cdot e(t_1) \cdot h \cdot \frac{\partial f(t_0, y_{u_0}(t_0), u_0)}{\partial u_0} \quad (23)$$

$$u_1 = u_0 + \lambda \cdot e(t_1) \cdot \frac{\partial y_{u_0}(t_1)}{\partial u_0} \quad (24)$$

In general case, it is difficult to calculate the expression of $\frac{\partial y_{u_0}(t_1)}{\partial u_0}$, therefore, it has been known that the neural network can approximate any nonlinear function, then, it can be used to approximate $\frac{\partial y_{u_0}(t_1)}{\partial u_0}$.

3.1 RBF neural network algorithm

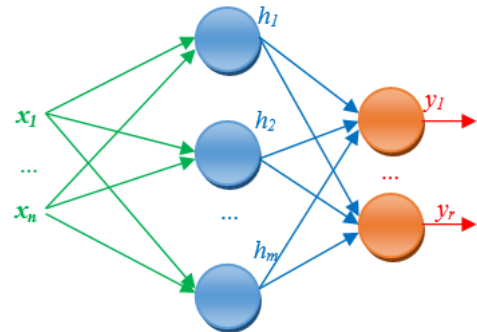


Figure 5. RBF neural network structure

A radial basis function neural network (RBFNN) is introduced into neural network in the paper [13], it has three layers: an input layer, a nonlinear hidden layer that uses Gaussian function as activation function, and a linear output layer [14]. The RBF networks have many uses, including function approximation, classification, and system control. It has the advantage of fast learning speed and is able to avoid the problem of local minimum.

The structure of the RBF neural network is illustrated in Figure 5.

The output of the j^{th} hidden neurons is given by the following equation:

$$h_j = \exp\left(-\frac{\|X - C_{i,j}\|^2}{2b_j^2}\right) \quad (25)$$

where, $X = [x_1, x_2, \dots, x_n]^T$ is the input vector of the neural network.

The RBF neural network output is described in the following equation:

$$y_{RBFNN} = \sum_{j=1}^m W_{l,j} h_j = \sum_{j=1}^m W_{l,j} \exp\left(-\frac{\|X - C_{i,j}\|^2}{2b_j^2}\right) \quad (26)$$

where, $W_{l,j}$ is the weight between the hidden layer and the output layer. The center $C_{i,j}$, the basis width parameter b_j and the weights $W_{l,j}$ of the RBF neuron network are adjusted by using the gradient descent algorithm to minimize the sum of square error E_{RBFNN} .

The expression of E_{RBFNN} is given as follow:

$$E_{RBFNN} = \frac{1}{2} \sum (e_{RBFNN}(k))^2 = \frac{1}{2} \sum_{k=1}^r (y_{u_k}(k) - y_{RBFNN}(k))^2 \quad (27)$$

$$C_{i,j}(k) = C_{i,j}(k-1) + \Delta C_{i,j} + \alpha(C_{i,j}(k-1) - C_{i,j}(k-2)) \quad (28)$$

$$b_j(k) = b_j(k-1) + \Delta b_j + \alpha(b_j(k-1) - b_j(k-2)) \quad (29)$$

$$W_{l,j}(k) = W_{l,j}(k-1) + \Delta W_{l,j} + \alpha(W_{l,j}(k-1) - W_{l,j}(k-2)) \quad (30)$$

The corresponding modifier formulas are as follows:

$$\Delta C_{i,j} = -\eta \frac{\partial E_{RBFNN}}{\partial C_{i,j}} = -\eta \frac{\partial E_{RBFNN}}{\partial y_{RBFNN}} \frac{\partial y_{RBFNN}}{\partial h_j} \frac{\partial h_j}{\partial C_{i,j}} \quad (31)$$

$$\Delta C_{i,j} = \eta \cdot e_{RBF} W_{l,j} h_j \cdot \left(\frac{X - C_{i,j}}{b_j^2}\right) \quad (32)$$

$$\Delta b_j = -\eta \frac{\partial E_{RBFNN}}{\partial b_j} = -\eta \frac{\partial E_{RBFNN}}{\partial y_{RBFNN}} \frac{\partial y_{RBFNN}}{\partial h_j} \frac{\partial h_j}{\partial b_j} \quad (33)$$

$$\Delta b_j = \eta \cdot e_{RBFNN} W_{l,j} h_j \cdot \frac{\|X - C_{i,j}\|^2}{b_j^3} \quad (34)$$

$$\Delta W_{l,j} = -\eta \frac{\partial E_{RBFNN}}{\partial W_{l,j}} = -\eta \frac{\partial E_{RBFNN}}{\partial y_{RBFNN}} \frac{\partial y_{RBFNN}}{\partial W_{l,j}} \quad (35)$$

$$\Delta W_{l,j} = \eta \cdot e_{RBFNN} \cdot h_j \quad (36)$$

where, α is the momentum factor, and η is the learning rate. From Eq. (24), we have:

$$u_1 = u_0 + \lambda \cdot e(t_1) \cdot \frac{\partial y_{u_0}(t_1)}{\partial u_0} \quad (37)$$

The RBF neural network will be used to calculate the expression of $\frac{\partial y_{u_0}(t_1)}{\partial u_0}$.

The schema of RBF neural network identification is depicted in Figure 6.

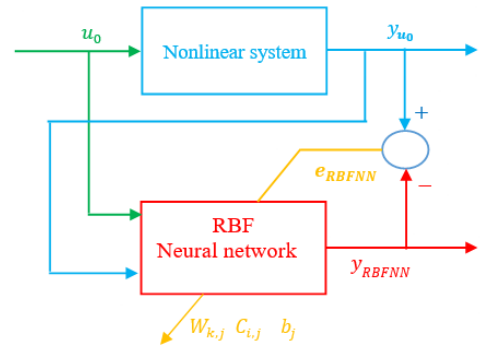


Figure 6. Schema of RBF neural network identification

If the RBF neural network output y_{RBFNN} is equal to the system output y_{u_0} [15, 16], then, we can use the expression of

$$y_{RBFNN} \text{ to calculate the expression of } \frac{\partial y_{u_0}(t_1)}{\partial u_0}.$$

$$\frac{\partial y_{u_0}(t_1)}{\partial u_0} \approx \frac{\partial y_{RBFNN}}{\partial u_0} = \frac{\partial}{\partial u_0} \sum_{j=1}^r W_{l,j} h_j \quad (38)$$

$$\frac{\partial y_{u_0}(t_1)}{\partial u_0} = \frac{\partial}{\partial u_0} \sum_{j=1}^r W_{l,j} \exp\left(-\frac{\|X - C_{i,j}\|^2}{2b_j^2}\right) \quad (39)$$

$$\frac{\partial y_{u_0}(t_1)}{\partial u_0} = \sum_{j=1}^r W_{l,j} \frac{\partial}{\partial u_0} \exp\left(-\frac{\|X - C_{i,j}\|^2}{2b_j^2}\right) \quad (40)$$

$$\frac{\partial y_{u_0}(t_1)}{\partial u_0} = \sum_{j=1}^r W_{l,j} \frac{\partial}{\partial x_1} \exp\left(-\frac{X^T X - X^T C_{i,j} - C_{i,j}^T X + C_{i,j}^T C_{i,j}}{2b_j^2}\right) \quad (41)$$

$$\text{With: } X = [u_0 \quad y_{u_0}]^T = [x_1 \quad x_2]^T$$

$$C_{i,j} = \begin{bmatrix} C_{1,1} & C_{1,2} & \dots & C_{1,m} \\ C_{2,1} & C_{2,2} & \dots & C_{2,m} \end{bmatrix}$$

$$\frac{\partial y_{u_0}(t_1)}{\partial u_0} = \sum_{j=1}^r W_{1,j} \frac{\partial}{\partial x_1} \exp \left(\frac{[x_1 \ x_2] \begin{bmatrix} x_1 \\ x_2 \end{bmatrix} - [x_1 \ x_2] C_{i,j} - C_{i,j}^T \begin{bmatrix} x_1 \\ x_2 \end{bmatrix} + C_{i,j}^T C_{i,j}}{2b_j^2} \right) \quad (42)$$

$$\frac{\partial y_{u_0}(t_1)}{\partial u_0} = \sum_{j=1}^r W_{1,j} \frac{\partial}{\partial x_1} \exp \left(- \frac{x_1^2 + x_2^2 - 2x_1 C_{1,j} - 2x_2 C_{2,j} + C_{i,j}^T C_{i,j}}{2b_j^2} \right) \quad (43)$$

$$\frac{\partial y_{u_0}(t_1)}{\partial u_0} = \sum_{j=1}^r W_{1,j} \left(\frac{C_{1,j} - x_1}{b_j^2} \right) \exp \left(- \frac{x_1^2 + x_2^2 - 2x_1 C_{1,j} - 2x_2 C_{2,j} + C_{i,j}^T C_{i,j}}{2b_j^2} \right) \quad (44)$$

So:

$$\frac{\partial y_{u_0}(t_1)}{\partial u_0} = \sum_{j=1}^r W_{1,j} \left(\frac{C_{1,j} - x_1}{b_j^2} \right) h_j \quad (45)$$

We substitute Eq. (45) in Eq. (37) to get the control law:

$$u_1 = u_0 + \lambda \cdot e(t_1) \cdot \sum_{j=1}^r W_{1,j} \left(\frac{C_{1,j} - x_1}{b_j^2} \right) h_j \quad (46)$$

The steps of the proposed control strategy are as follows:

Step1. We start by $u=u_0$ (the choice of u_0 depend on the study system).

Step2. Initializing the network parameters: the number of nodes in input, hidden and output layer, the center $C_{i,j}$, the basis width parameter b_j and the weights $W_{i,j}$, learning rate.

Step3. for $k \geq 0$.

- Calculating the output $y_{u_k}(t_{k+1})$ and network output $y_{RBFNN}(t_{k+1})$, calculating the error $e_{RBFNN}(t_{k+1})$.

- Adjusting of neural network parameters: $C_{i,j}$, b_j and $W_{i,j}$ from Eq. (32), Eq. (34) and Eq. (36).

- Calculating error $e(t_{k+1})$ between $y_{u_k}(t_{k+1})$ and $r(t_{k+1})$.

- Calculating the new value of u_{k+1} via the following expression:

$$u_{k+1} = u_k + \lambda \cdot e(t_{k+1}) \cdot \sum_{j=1}^r W_{1,j} \left(\frac{C_{1,j} - x_1}{b_j^2} \right) h_j \quad (47)$$

Step 4. We replace the found value of u_{k+1} on the system.

$$y_{u_0}(t_{k+1}) = y_{u_0}(t_k) + h \cdot f(t_k, y_{u_0}(t_k), u_{k+1}) \quad (48)$$

According to this algorithm, we can obtain: $y_{u_0}(t_{k+1}) = r(t_{k+1})$.

The structure of the proposed method is illustrated in Figure 7.

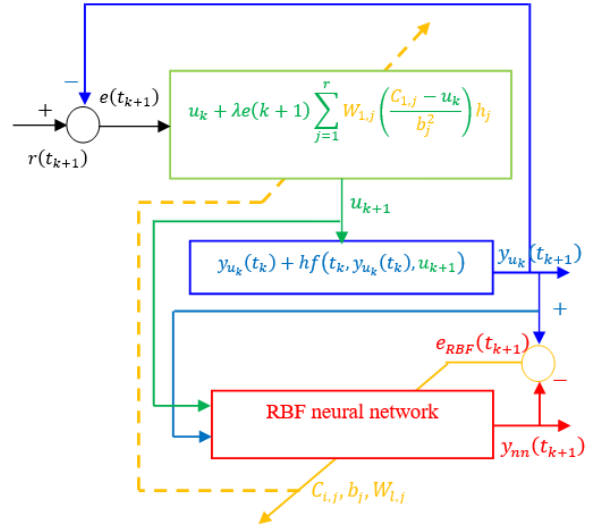


Figure 7. Schema of the proposed control strategy

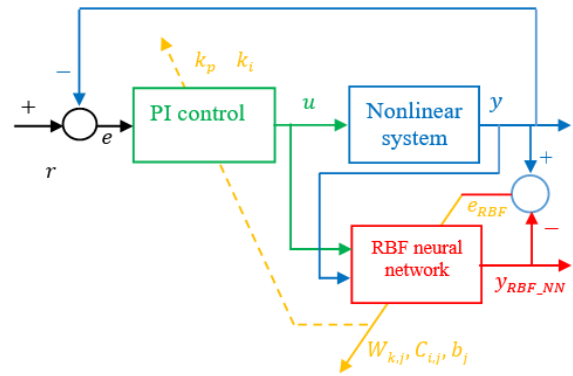


Figure 8. Adaptive RBF neural network PI structure

4. STRUCTURE OF RBF NEURAL NETWORK PI CONTROL

The structure of the RBF neural network PI is based on two control strategy (Figure 8), the first one is a conventional PI control because of its good control performance and the second is the RBF neural network control strategy. The PI control is used for controlling the dissolved oxygen concentration in the aerobic reactor, and the RBF neural network is used to regulate the parameters of PI control: k_p and k_i for improving the adaptability of the controller.

The mathematical expression of the PI (Proportional Integral) control algorithm is given by the following equation:

$$u(k) = u(k-1) + k_p(e(k) - e(k-1)) + k_i e(k) \quad (49)$$

where, $u(k)$ is the output of the PI control (the input control of the system) and e is the error between the desired output r and actual system output.

$$e(k) = r(k) - y(k) \quad (50)$$

It has been known that the PI control performance is based on the value of PI parameters k_p and k_i . To improve the performance of the PI controller against the disturbance on the system, the parameters k_p and k_i can be auto-adjusted and optimized, so, the adaptive PI control algorithm became:

$$u(k) = u(k-1) + k_p(k)(e(k) - e(k-1)) + k_i(k)e(k) \quad (51)$$

The parameters of PI controller (k_p and k_i) are adjusted (auto-tuning) by using the gradient descent algorithm to minimize the sum of squared error E between the system output y and the desired output r .

The performance function E is defined as:

$$E(k) = \frac{1}{2} \sum_{k=1}^N (r(k) - y(k))^2 = \frac{1}{2} \sum_{k=1}^N (e(k))^2 \quad (52)$$

According to the gradient descent method, the adjustment rules of the PI parameters are given as:

$$k_p(k) = k_p(k-1) + \Delta k_p \quad (53)$$

$$k_i(k) = k_i(k-1) + \Delta k_i \quad (54)$$

where,

$$\Delta k_p = -\eta \frac{\partial E}{\partial k_p} = -\eta \frac{\partial E}{\partial y} \frac{\partial y}{\partial u} \frac{\partial u}{\partial k_p} = \eta e(k) \frac{\partial y}{\partial u} (e(k) - e(k-1)) \quad (55)$$

$$\Delta k_i = -\eta \frac{\partial E}{\partial k_i} = -\eta \frac{\partial E}{\partial y} \frac{\partial y}{\partial u} \frac{\partial u}{\partial k_i} = \eta e(k) \frac{\partial y}{\partial u} e(k) \quad (56)$$

where,

$$\frac{\partial y}{\partial u} = \sum_{j=1}^r W_{1,j} \left(\frac{C_{1,j} - x_1}{b_j^2} \right) h_j \quad (57)$$

5. MATHEMATICAL MODEL OF WASTEWATER TREATMENT PROCESS

The schematic of the wastewater treatment process is represented in Figure 9.

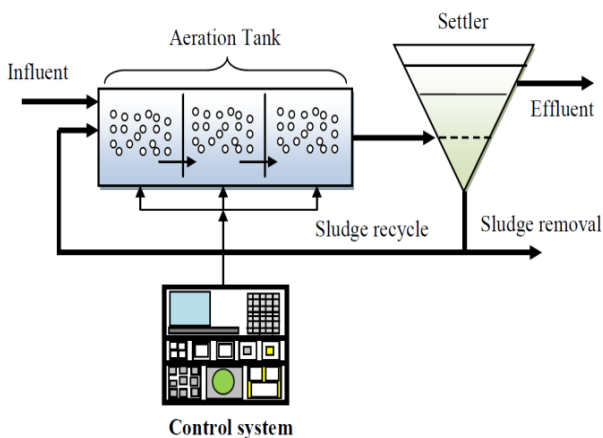


Figure 9. Schema of activated sludge process

The aeration tank is a biological reactor in which the microorganisms are developed by removing the organic substrate in the presence of the dissolved oxygen concentration. In the settler tank the solids are separated from the wastewater. The growth of micro-organisms (biomass) in the aeration tank is not sufficient, then, a part of the removed sludge (the sludge contains the biomass) is recycled back to the aeration tank while the other part is removed from the system.

The mathematical model considered in this paper contains four differential equations, the biomass concentration X , the substrate concentration S , the dissolved oxygen concentration DO and the recycled biomass concentration X_r . The model is given by the following equations [17, 18].

$$\frac{\partial X(t)}{\partial t} = \mu(t)X(t) - D(1+r)X(t) + rDX_r(t) \quad (58)$$

$$\frac{\partial S(t)}{\partial t} = -\frac{1}{Y} \mu(t)X(t) - D(1+r)S(t) + DS_{in} \quad (59)$$

$$\frac{\partial DO(t)}{\partial t} = -\frac{K_0}{Y} \mu(t)X(t) - D(1+r)DO(t) + KLa(DO_{max} - DO(t)) + DDO_{in} \quad (60)$$

$$\frac{\partial X_r(t)}{\partial t} = D(1+r)X(t) - D(\beta+r)X_r(t) \quad (61)$$

With:

$$\mu(t) = \mu_{max} \cdot \frac{S(t)}{S(t) + k_s} \cdot \frac{DO(t)}{DO(t) + k_{DO}} \quad (62)$$

$$KLa = \alpha W(k).$$

W : the aeration flow rate.

The aeration rate W is considered in this paper as the variable control for controlling the oxygen concentration in the aeration tank. Table 2 and Table 3 below show the parameters and initial values of the model respectively.

Table 2. Model parameters

Description	Parameters	Units	Values
Biomass yield factor	Y_h	-	0.65
Maximum specific growth rate	μ_{max}	h^{-1}	0.15
Half-saturation coefficient for micro-organisms	k_s	$mg.l^{-1}$	100
Oxygen half-saturation coefficient for micro-organisms	k_{DO}	$mg.l^{-1}$	2
Maximum DO concentration	DO_{max}	$mg.l^{-1}$	10
Model constant	K_0	-	0.5
Oxygen transfer rate	α	-	0.018
Ratio of recycled	r	-	0.6
Ratio of waste flow	β	-	0.2
Influent substrate concentration	S_{in}	$mg.l^{-1}$	200
Influent DO concentration	DO_{in}	$mg.l^{-1}$	0.5
Oxygen mass transfer coefficient	KLa	h^{-1}	-
Aeration rate	W	$m^3.h^{-1}$	-
Dilution rate	D	h^{-1}	-

Table 3. Initial values

Variables concentrations	Symbols	Units	Values
Substrate concentration	S_s	$mg. l^{-1}$	88
Biomass concentration	X	$mg. l^{-1}$	20
Dissolved oxygen concentration	DO	$mg. l^{-1}$	2
Recycle biomass concentration	X_r	$mg. l^{-1}$	320

6. RESULTS AND DISCUSSION

This paper proposes a control strategy based on Euler and gradient method based on Radial basis function neural network (RBFNN) is used to control the organic substances concentration in the aeration tank through the control of the dissolved oxygen concentration.

Figures 10 and 11 show the dissolved oxygen and substrate concentration in open loop (no control technique is applied to control the dissolved oxygen concentration). We can see clearly that the substrate concentration exceeds the maximum allowable value $20mg.l^{-1}$, so, the control of the dissolved oxygen concentration became obligatory for having a substrate concentration below the standard limit.

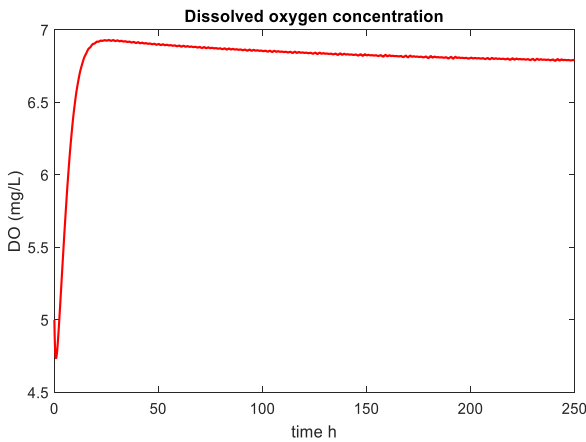


Figure 10. Dissolved oxygen concentration

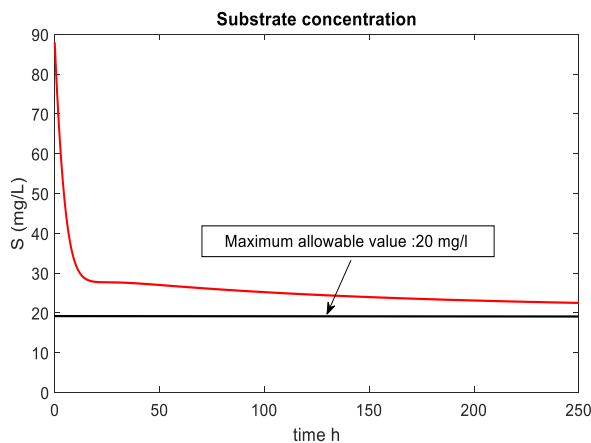


Figure 11. Substrate concentration

For comparison, RBF neural network PI controller has been used with the initial's parameters: $k_p=3$ and $k_i=0.9$.

The RBF neural network has the following structure (for the proposed control strategy and RB neural network PI control):

two inputs in input layer $X=[W DO]^T$, six neurons in hidden layer, and one neuron in output layer. The RBF neural network parameters C_{ij} , b_j and W_{kj} are respectively initialized in the range $[30, 60]$, $[20, 40]$, and $[0, 10]$, the learning rate $\mu=0.09$ and the momentum factor $\alpha=0.5$.

The step size $h=0.5$.

The dilution rate (Figure 12) is considered variable to cover many different regimes: high flow $D=0.035h^{-1}$, normal flow $D=0.025h^{-1}$ and low flow $D=0.015h^{-1}$. The influent substrate concentration S_{in} is also considered with different values to assure a real study of wastewater system (Figure 13).

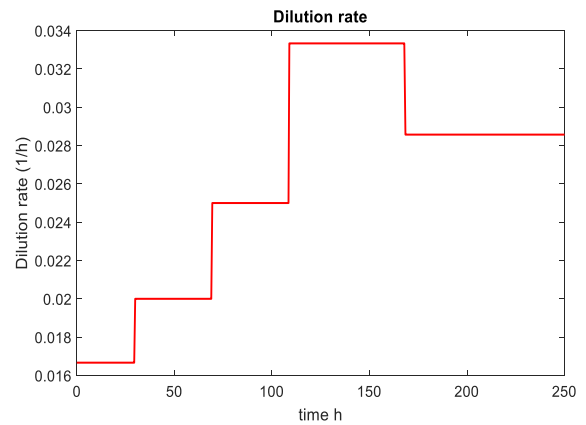


Figure 12. Dilution rate

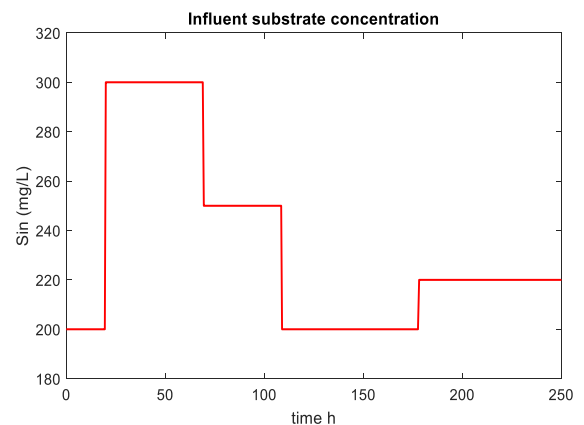


Figure 13. Influent substrate concentration

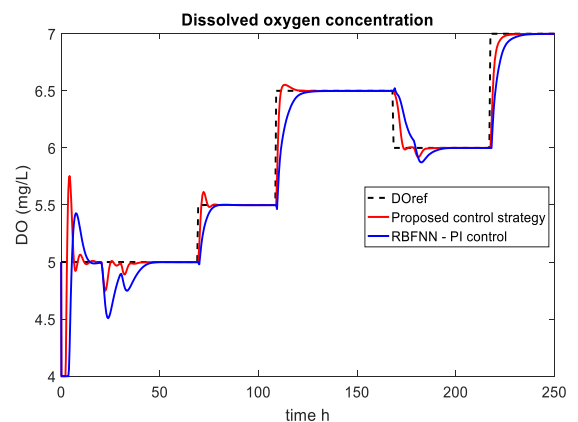


Figure 14. Dissolved oxygen concentration with modified dilution rate and influent substrate

From Figure 14, when the dilution rate and the influent substrate concentration changed, the RBFNN-PI controller is very affected by these changes and it is not well tracking the set-point reference DO_{ref} , contrary of the proposed method that is not very affected by these disturbances generated by dilution rate and the influent substrate concentration. The dissolved oxygen concentration has a good tracking of the set-point reference DO_{ref} by using the proposed control strategy. The aeration rate (control variable) is depicted in Figure 15.

Figure 16, shows clearly that substrate concentration is biologically degraded below the maximum allowable value $20mg.l^{-1}$.

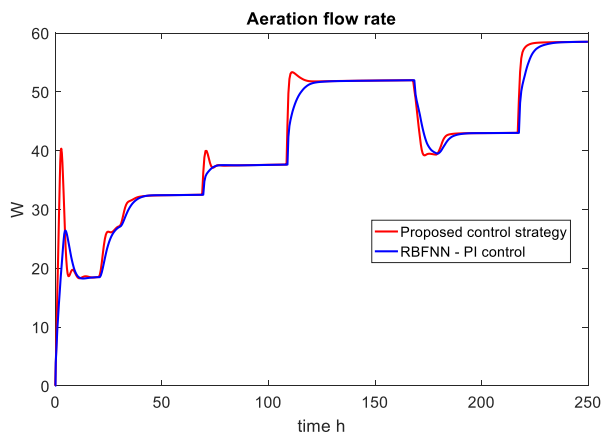


Figure 15. Aeration rate (Control variable)

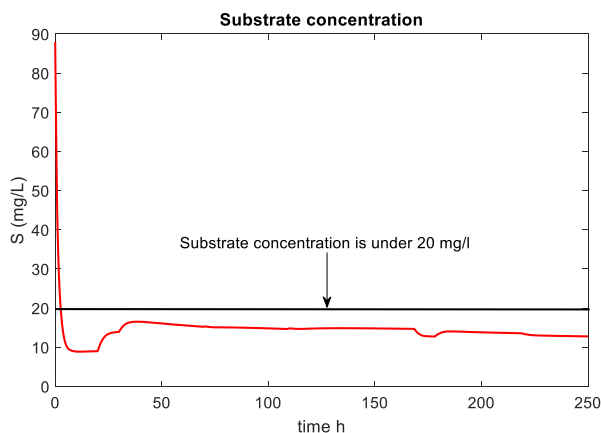


Figure 16. Substrate concentration

The criteria IAE (integral of absolute error) and ISE (integral of square error) are used to compare the performance of the different control strategies:

$$IAE = \int_0^{\infty} |e(t)| dt \quad (63)$$

$$ISE = \int_0^{\infty} e(t)^2 dt \quad (64)$$

The simulation results are compared from the view point of integral of absolute error (IAE). Considering this measure, the dissolved oxygen concentration has the best results applying the proposed controller (Table 1).

Table 1. Simulated IAE and ISE of the controllers

Used control methods	IAE	ISE
RBFNN-PI controller	0.1232	0.0740
Proposed controller	0.0678	0.0455

7. CONCLUSION

In this paper, an Euler control strategy and gradient method based on RBFNN has been established to control the substrate concentration via the control of the dissolved oxygen concentration in an activated sludge process of wastewater treatment. The effectiveness of the proposed method was evaluated through a comparison with RBF neural network PI controller. The simulation results indicate that the proposed control strategy has a better performance for tracking the set-point reference DO_{ref} compared to the RBF neural network PI control.

REFERENCES

- [1] Babuponnusami, A., Muthukumar, K. (2014). A review on Fenton and improvements to the Fenton process for wastewater treatment. *Journal of Environmental Chemical Engineering*, 2(1): 557-572. <https://doi.org/10.1016/j.scitotenv.2019.03.180>
- [2] Passos, F., Gutiérrez, R., Brockmann, D., Steyer, J.P., García, J., Ferrer, I. (2015). Microalgae production in wastewater treatment systems, anaerobic digestion and modelling using ADM1. *Algal Research*, 10: 55-63. <https://doi.org/10.1016/j.algal.2015.04.008>
- [3] Mannina, G., Ekama, G., Caniani, D., Cosenza, A., Esposito, G., Gori, R., Olsson, G. (2016). Greenhouse gases from wastewater treatment-A review of modelling tools. *Science of the Total Environment*, 551: 254-270. <https://doi.org/10.1016/j.scitotenv.2016.01.163>
- [4] Du, X., Wang, J., Jegatheesan, V., Shi, G. (2018). Dissolved oxygen control in activated sludge process using a neural network-based adaptive PID algorithm. *Applied Sciences*, 8(2): 261. <https://doi.org/10.3390/app8020261>
- [5] Holenda, B., Domokos, E., Rédey, Á., Fazakas, J. (2008). Dissolved oxygen control of the activated sludge wastewater treatment process using model predictive control. *Computers & Chemical Engineering*, 32(6): 1270-1278. <https://doi.org/10.1016/j.compchemeng.2007.06.008>
- [6] Man, Y., Shen, W., Chen, X., Long, Z., Corriou, J.P. (2018). Dissolved oxygen control strategies for the industrial sequencing batch reactor of the wastewater treatment process in the papermaking industry. *Environmental Science: Water Research & Technology*, 4(5): 654-662. <https://doi.org/10.1039/C8EW00035B>
- [7] Liu, D., Zong, X. (2019). Dissolved oxygen control in sewage treatment process based on fuzzy active disturbance rejection control. In *2019 IEEE 3rd Advanced Information Management, Communicates, Electronic and Automation Control Conference (IMCEC)*, pp. 1164-1168. <https://doi.org/10.1109/IMCEC46724.2019.8983931>
- [8] Han, H., Liu, Z., Qiao, J. (2019). Fuzzy neural network-based model predictive control for dissolved oxygen

- concentration of WWTPs. *International Journal of Fuzzy Systems*, 21: 1497-1510. <https://doi.org/10.1007/s40815-019-00644-8>
- [9] Piotrowski, R. (2020). Supervisory fuzzy control system for biological processes in sequencing wastewater batch reactor. *Urban Water Journal*, 17(4): 325-332. <https://doi.org/10.1080/1573062X.2020.1778744>
- [10] Lin, M.J., Luo, F. (2016). Adaptive neural control of the dissolved oxygen concentration in WWTPs based on disturbance observer. *Neurocomputing*, 185: 133-141. <https://doi.org/10.1016/j.neucom.2015.12.045>
- [11] Han, H.G., Zhang, L., Liu, H.X., Qiao, J.F. (2018). Multiobjective design of fuzzy neural network controller for wastewater treatment process. *Applied Soft Computing*, 67: 467-478. <https://doi.org/10.1016/j.asoc.2018.03.020>
- [12] Mirghasemi, S., Macnab, C.J.B., Chu, A. (2014). Dissolved oxygen control of activated sludge bioreactors using neural-adaptive control. In *Proceedings of the IEEE Symposium on Computational Intelligence in Control and Automation (CICA 2014)*, Orlando, FL, USA, pp. 9-12. <https://doi.org/10.1109/CICA.2014.7013237>
- [13] Macnab, C.J.B. (2014). Stable neural-adaptive control of activated sludge bioreactors. In *Proceedings of the 2014 American Control Conference (ACC2014)*, Portland, OR, USA, pp. 4-6. <https://doi.org/10.1109/ACC.2014.6858627>
- [14] Qiao, J.F., Hou, Y., Zhang, L., Han, H.G. (2018). Adaptive fuzzy neural network control of wastewater treatment process with multiobjective operation. *Neurocomputing*, 275: 383-393. <https://doi.org/10.1016/j.neucom.2017.08.059>
- [15] Han, H.G., Qiao, J.F., Chen, Q.L. (2012). Model predictive control of dissolved oxygen concentration based on a self-organizing RBF neural network. *Control Engineering Practice*, 20(4): 465-476. <https://doi.org/10.1016/j.conengprac.2012.01.001>
- [16] Ruan, J., Zhang, C., Li, Y., Li, P., Yang, Z., Chen, X., Huang, M., Zhang, T. (2017). Improving the efficiency of dissolved oxygen control using an on-line control system based on a genetic algorithm evolving FWNN software sensor. *Journal of Environmental Management*, 187: 550-559. <https://doi.org/10.1016/j.jenvman.2016.10.056>
- [17] Belchior, C.A.C., Araújo, R.A.M., Landeck, J.A.C. (2012). Dissolved oxygen control of the activated sludge wastewater treatment process using stable adaptive fuzzy control. *Computers & Chemical Engineering*, 37: 152-162. <https://doi.org/10.1016/j.compchemeng.2011.09.011>
- [18] Jeppsson, U., Rosen, C., Alex, J., Copp, J., Gernaey, K.V., Pons, M.N., Vanrolleghem, P.A. (2006). Towards a benchmark simulation model for plant-wide control strategy performance evaluation of WWTPs. *Water Sci. Technol*, 53(1): 287-295. <https://doi.org/10.2166/wst.2006.031>